Supporting information

Low-Power Driven Broadband Phototransistor with a $PbS/IGO/HfO_2$ Stack

*Hongwei Xu, Hee Sung Han, Jae Seok Hur, Min Jae Kim,Cheol Hee Choi,Taikyu Kim, Joon-Hyuk Chang, and Jae KyeongJeong**

Department of Electronic Engineering, Hanyang University, Seoul 04763, South Korea

Corresponding Author

*E-mail: jkjeong1@hanyang.ac.kr

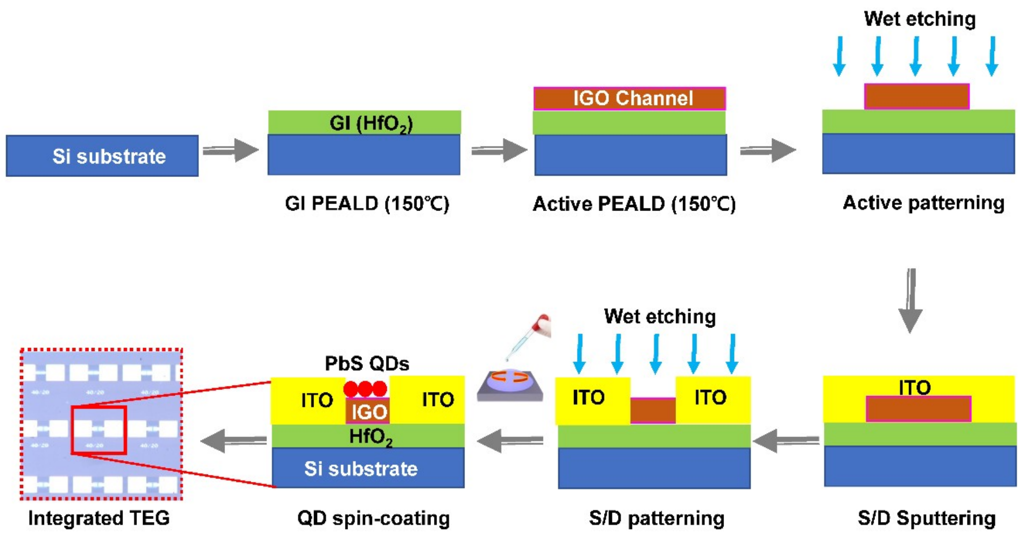

Figure S1. The schematic integration flow chart of phototransistors with the $PbS/IGO/HfO_2$ stack. The width of S/D electrode was larger than that of channel island region by ~10 %. Because the channel width as a *W* value was used in calculating the field-effect mobility, the mobility overestimation due to the fringe effect can be mitigated.

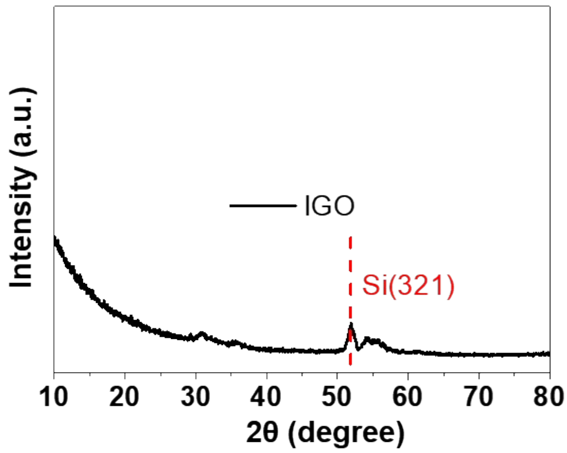

Figure S2. XRD pattern of the IGO thin film

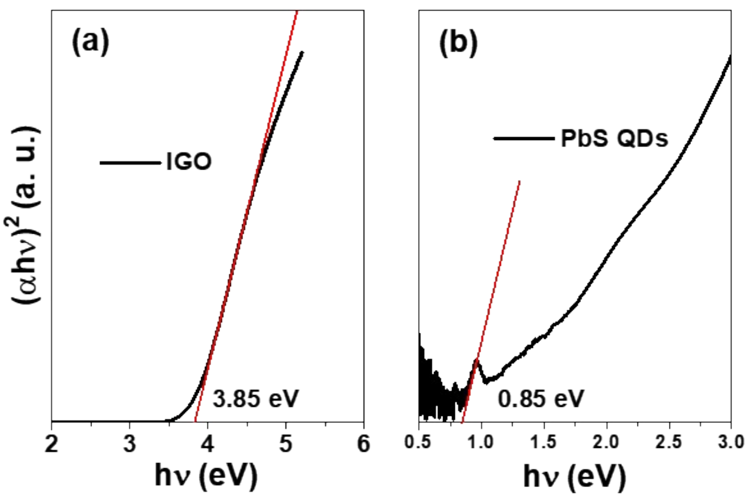

Figure S3. Tauc plots for energy band gap of IGO and PbS QDs films.

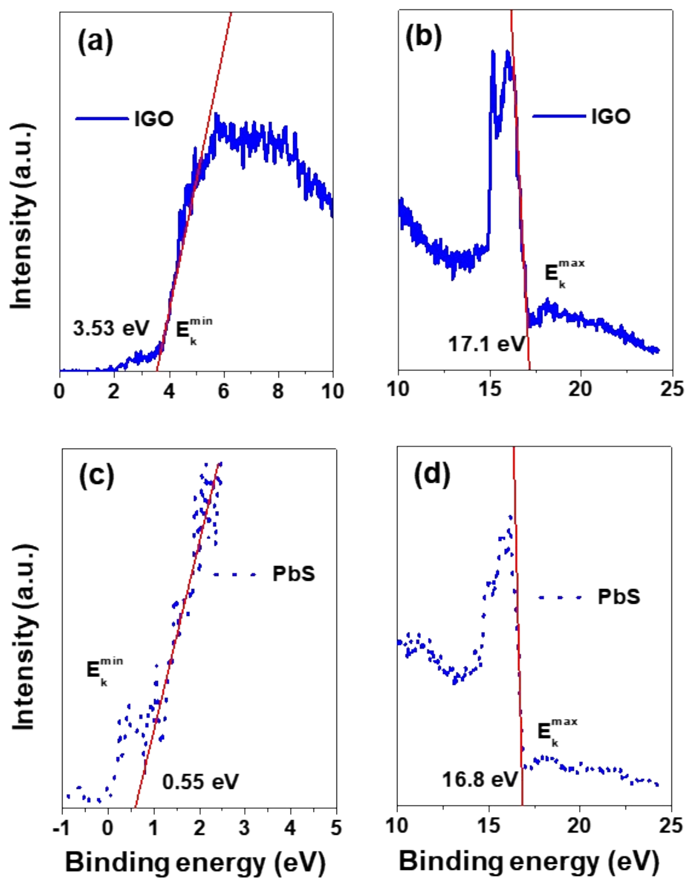

Figure S4. UPS analysis of IGO and PbS QDs films.

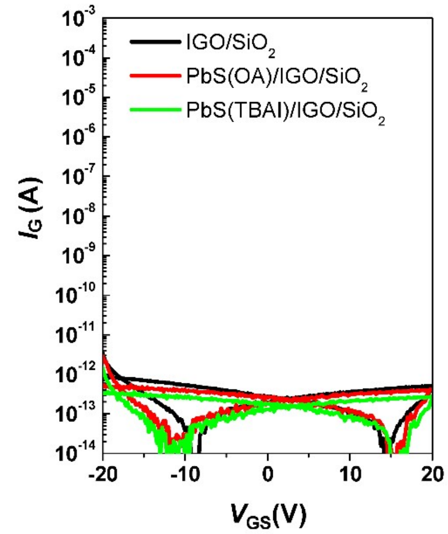

Figure S5. Comparison of gate leakage current characteristics for the TFTs with IGO, PbS(OA)/IGO, and PbS(TBAI)/IGO stacks on the SiO_2/Si substrate.

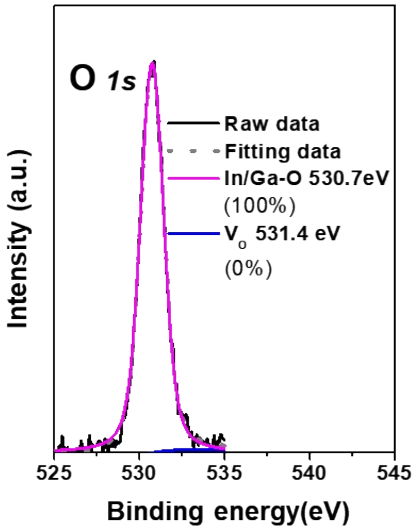

Figure S6. O*1s* XPS of IGO layer

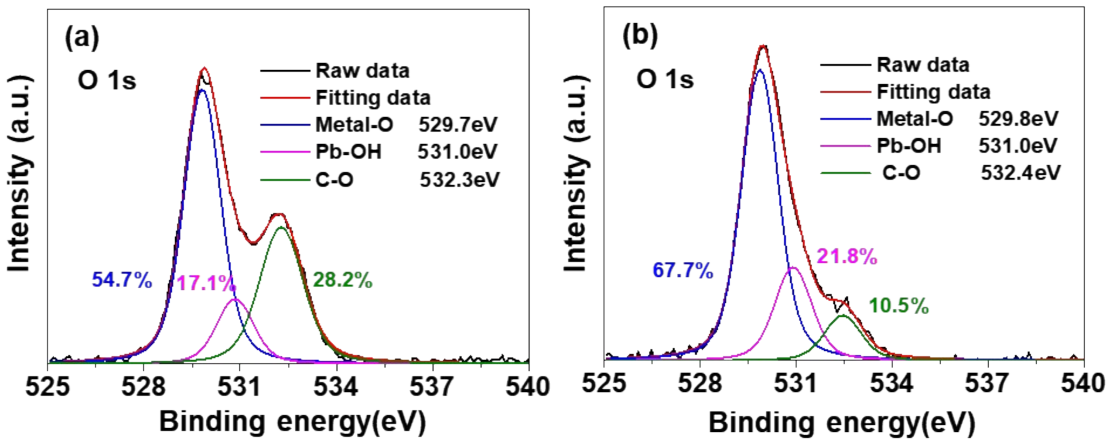

Figure S7. O*1s* XPS near the interface of (a) Pb-OA/IGO layer and (b) Pb-TBAI/IGO layer.

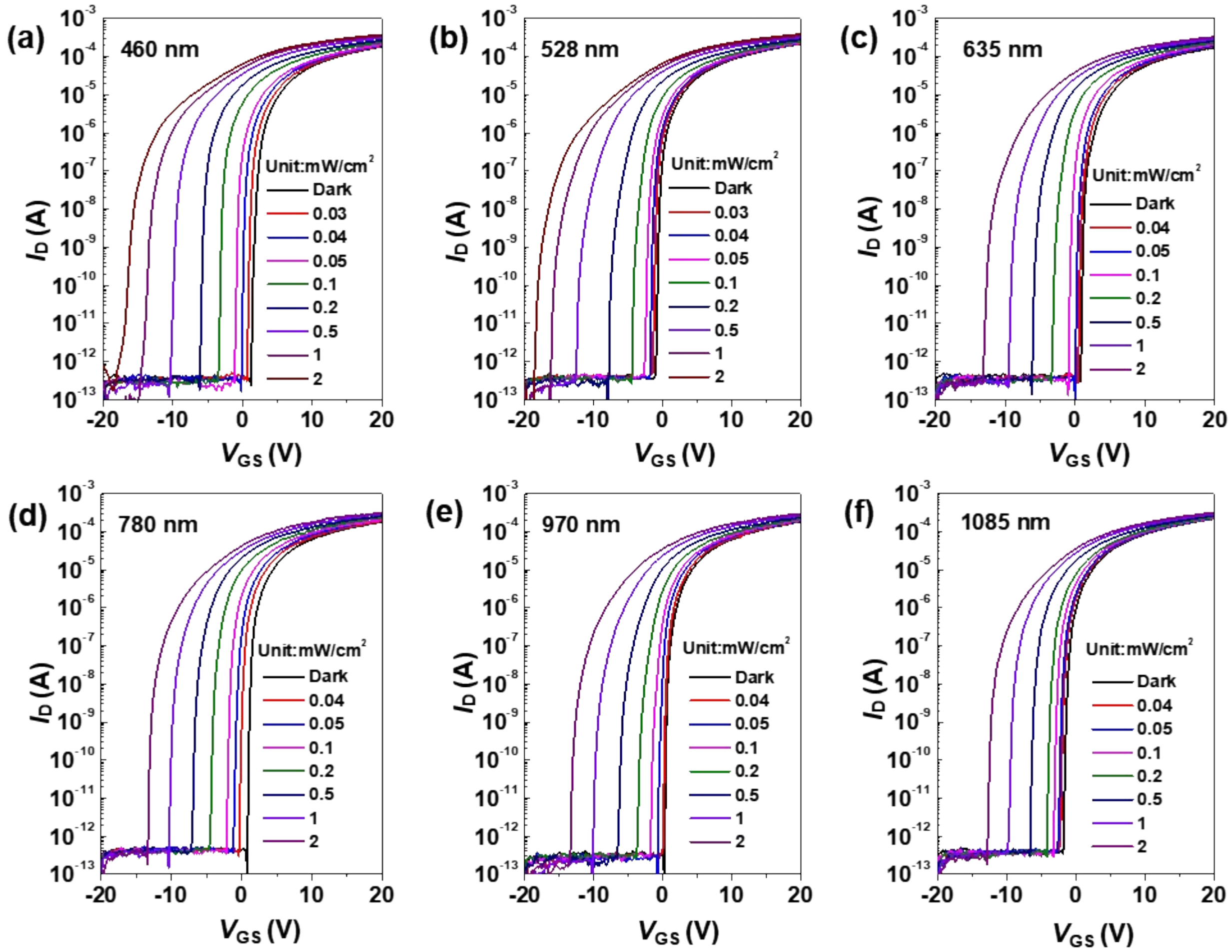

Figure S8. Transfer characteristics of PbS(TBAI)/IGO/SiO_2 phototransistors under photo-exposures at $\lambda = 460$, 528, 635, 780, 970, and 1085 nm.

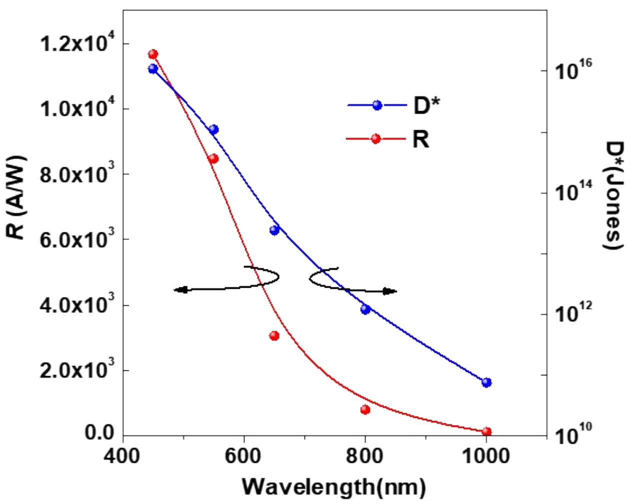

Figure S9. *R* and *D** of the PbS(OA)/IGO phototransistors as a function of incident light wavelength.

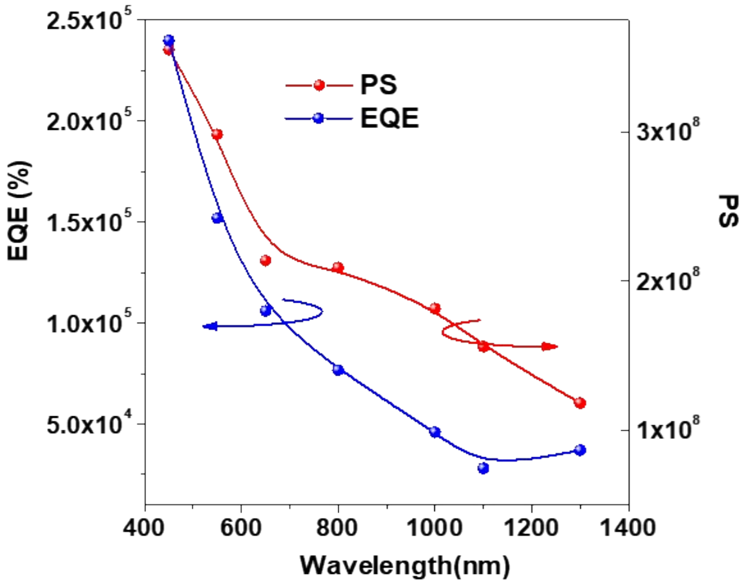

Figure S10. *PS* and *EQE* of the PbS(TBAI)/IGO phototransistors as a function of incident light wavelength.

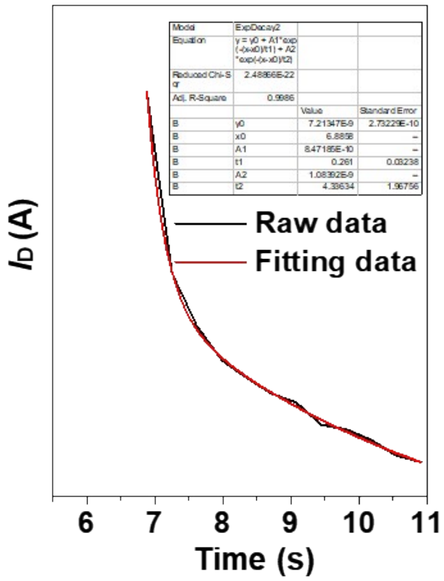

Figure S11. Transient current variation of PbS(TBAI)/IGO phototransistors under NIR exposure (λ = 1300 nm).

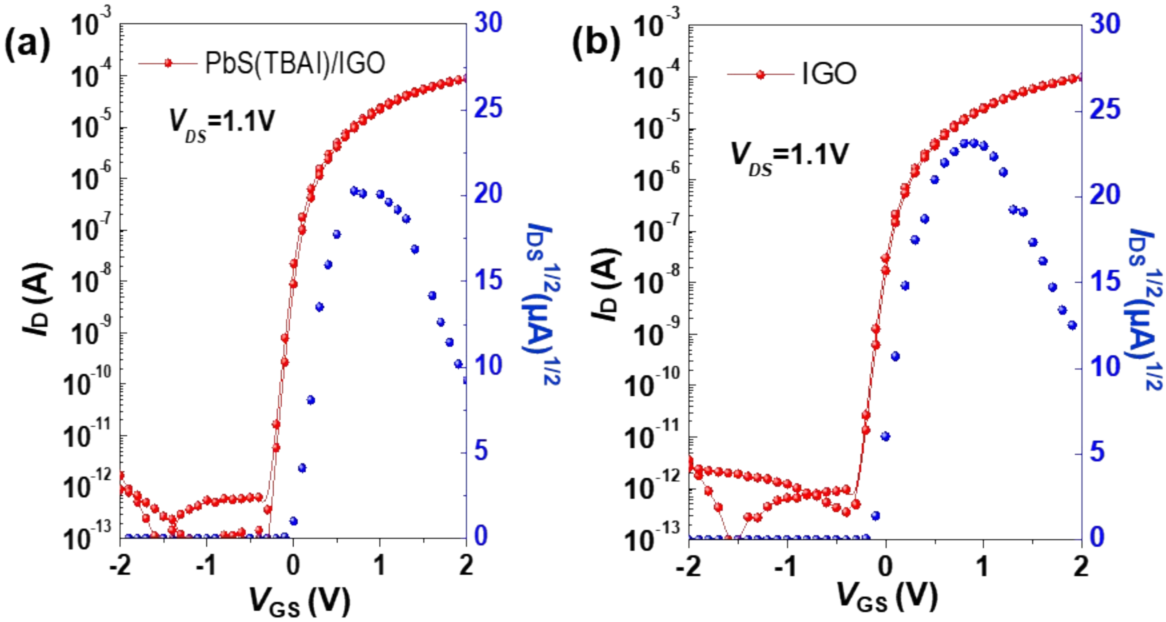

Figure S12. Transfer characteristics of phototransistors with (a) IGO and (b) PbS(TBAI)/IGO/HfO_2 stack in the dark.

Table S1. Comparisons of electrical parameters of phototransistors with n-type stack channel.

P-N junction	*W/L* (μm)	Method	V_{TH} (V)	$I_{ON/OFF}$ ratio	μ_{SAT} (cm^2/V.s)	*SS* (V/dec)	Operation Voltage(V)		Ref
							V_{DS}	V_{GS}	
IGZO(SnO)	800/500	Sputter	3.4	1.5×10^7	2.0	0.50	20	-10~20	**[1]**
IGZO(MoS_2)	100/50	Sputter	-	10^7<	-	-	10	-40~40	**[2]**
IGZO(PVK)	600/60	Sputter	-0.33	10^4	-	1.92	2	-15~20	**[3]**
IGZO(PVK)	80/80	Sputter	-	10^5	-	-	2	-10~10	**[4]**
IGZO(Polymer)	500/30	Sputter	28	10^9	16	0.60	5	-30~40	**[5]**
IGZO(PbS)	200/25	Sputter	>10	10^5	-	-	2	0~30	**[6]**
IGZO(CdSe/PbS)	100/50	Solution	-	10^9	10.75	0.726	15	-15~15	**[7]**
SIZO(QDs)	250/50	Sputter	~ -20	10^7	10	-	5	-30~60	**[8]**
IGZO(PbS)	1000/50	Sputter	1.68	10^8	13.10	-	20	-20~20	**[9]**
IGZO(PbS)	900/50	Sputter	>1	10^8<	6.36	-	5	-3~7	**[10]**
IGZO($CsPbBr_3$)	100/100	Sputter	2.27	2.7×10^8	8.95	0.52	30	-20~30	**[11]**
IGZO(ZnO)	100/20	Sputter	>2	10^5			10	-10~18	**[12]**
IZO(BHJ)	1000/30	Solution	-	10^6	0.83	-	5	-40~40	**[13]**
IGZO(Se)	1000/150	Sputter	-1.71	6.5×10^9	6.72	0.31	10.1	-30~30	**[14]**
IGZO(PVK)	1000/150	Sputter	-	10^8	-	-	10.1	-30~30	**[15]**
IGO(PbS)	40/20	PEALD	0.68	1.5×10^9	26.8	0.125	5.1	-20~20	**This work**
IGO(PbS)	40/20	PEALD	0.02	2.2×10^8	20.1	0.06	1.1	-2~2	

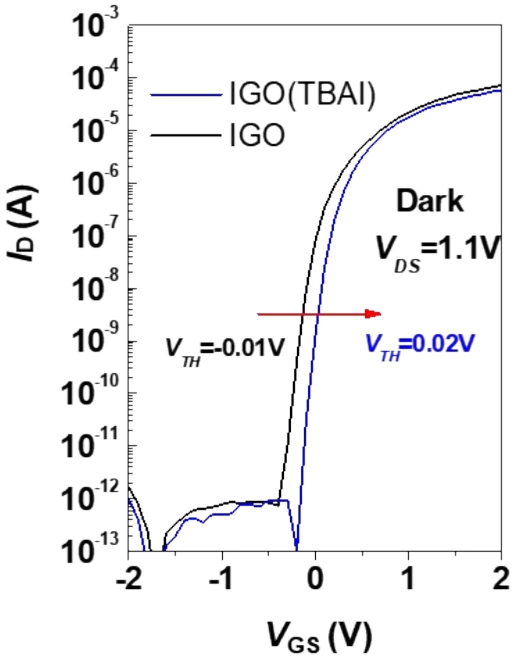

Figure S13. Comparison of transfer characteristics of the IGO/HfO_2 and PbS(TBAI)/IGO/HfO_2 transistors in the dark condition.

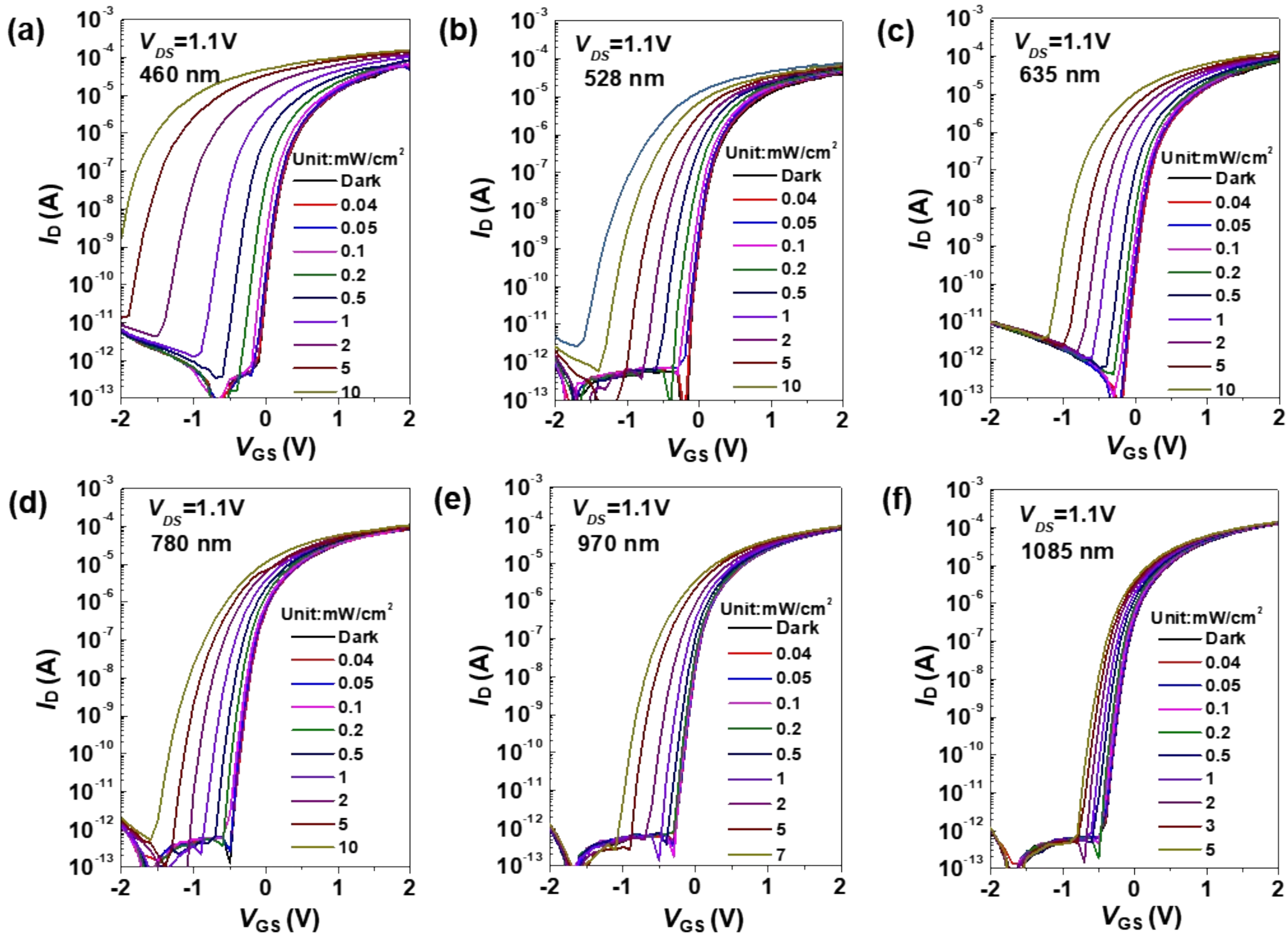

Figure S14. Photo-response of transfer characteristics of PbS(TBAI)/IGO/HfO_2 phototransistors under photo-exposure (λ = 460, 528, 635, 780, 970, and 1085 nm).

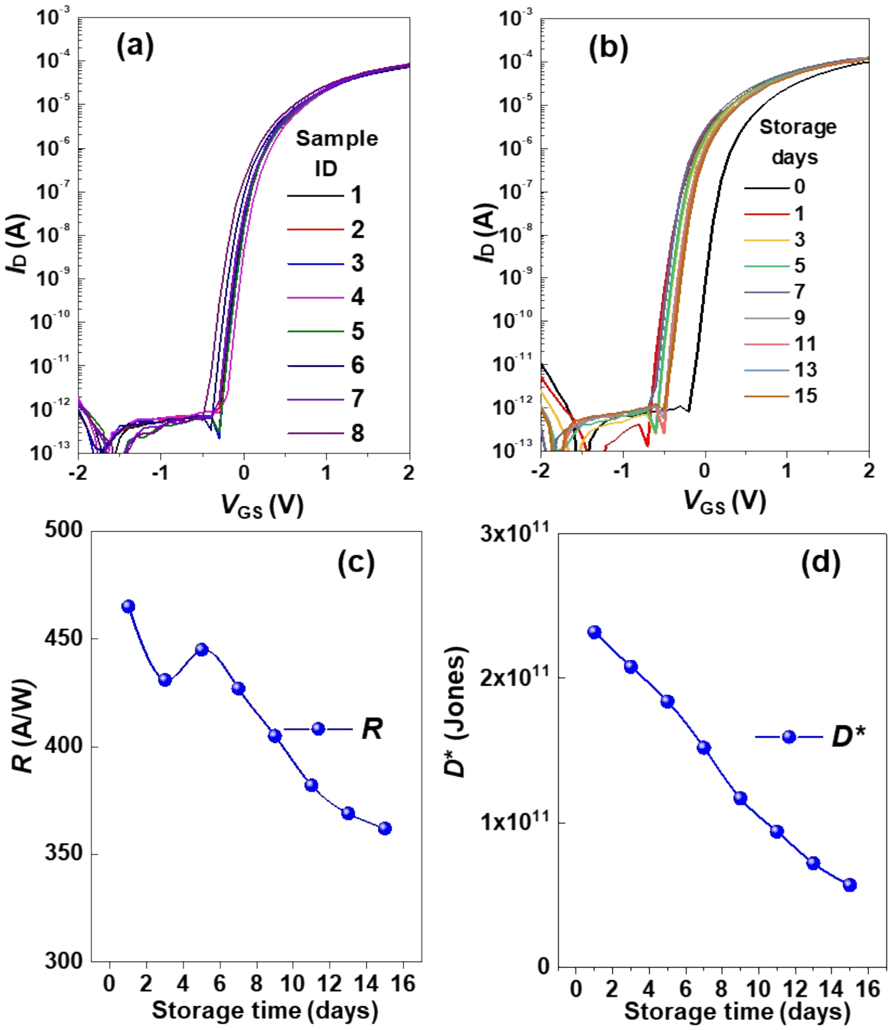

Figure S15 (a) The collected transfer characteristics of the PbS(TBAI)/IGO/HfO_2 phototransistors in different batches. (b) The stability of the transfer characteristics of the PbS(TBAI)/IGO/HfO_2 phototransistors under 1300 nm light illumination (3.3 mW/cm^2) within 15 days.

Reference

[1] J. Yu, K. Javaid, L. Liang, W. Wu, Y. Liang, A. Song, et al., High-performance visible-blind ultraviolet photodetector based on IGZO tft coupled with p-n heterojunction, ACS Appl Mater Interfaces, 10(2018) 8102-9.

[2] J. Yang, H. Kwak, Y. Lee, Y. S. Kang, M. H. Cho, J. H. Cho, et al., MoS_2-InGaZnO Heterojunction phototransistors with broad spectral responsivity, ACS Appl Mater Interfaces, 8(2016) 8576-82.

[3] X. Xu, L. Yan, T. Zou, R. Qiu, C. Liu, Q. Dai, et al., Enhanced Detectivity and Suppressed Dark Current of Perovskite-InGaZnO Phototransistor via a PCBM Interlayer, ACS Appl Mater Interfaces, 10(2018) 44144-51.

[4] S. Wei, F. Wang, X. Zou, L. Wang, C. Liu, X. Liu, et al., Flexible quasi-2D perovskite/IGZO phototransistors for ultrasensitive and broadband photodetection, Adv Mater, 32(2020) 1907527.

[5] Y. Wang, L. Wang, F. Liu, Z. Peng, Y. Zhang, C. Jiang, Organic-Inorganic Hybrid Heterostructures towards Long-Wavelength Photodetectors Based on InGaZnO-Polymer, Org Electron, 83(2020) 105778.

[6] S.W. Shin, K.H. Lee, J.S. Park, S.J. Kang, Highly Transparent, Visible-Light Photodetector Based on Oxide Semiconductors and Quantum Dots, ACS Appl Mater Interfaces, 7(2015) 19666-71.

[7] J. Kim, S.-M. Kwon, Y. K. Kang, Y.-H. Kim, M.-J. Lee, K. Han, et al., A skin-like two-dimensionally pixelized full-color quantum dot photodetector, Sci Adv, 5(2019) eaax8801.

[8] K. S. Cho, K. Heo, C. W. Baik, J. Y. Choi, H. Jeong, S. Hwang, et al., Color-selective photodetection from intermediate colloidal quantum dots buried in amorphous-oxide semiconductors, Nat Commun, 8(2017) 840.

[9] D. K. Hwang, Y. T. Lee, H. S. Lee, Y. J. Lee, S. H. Shokouh, J.-H. Kyhm, et al., Ultrasensitive PbS quantum-dot-sensitized InGaZnO hybrid photoinverter for near-Infrared detection and imaging with high photogain, NPG Asia Mater, 8(2016) e233.

[10] H. T. Choi, J.-H. Kang, J. Ahn, J. Jin, J. Kim, S. Park, et al., Zero-Dimensional PbS Quantum Dot–InGaZnO Film Heterostructure for Short-Wave Infrared Flat-Panel Imager, ACS Photonics, 7(2020) 1932-41.

[11] H. Yu, X. Liu, L. Yan, T. Zou, H. Yang, C. Liu, et al., Enhanced UV–visible detection of InGaZnO phototransistors via $CsPbBr_3$ quantum dots, Semicond Sci Tech, 34(2019) 125013.

[12] Z. Tao, X. Liu, W. Lei, J. Chen, High sensitive solar blind phototransistor based on ZnO nanorods/IGZO heterostructure annealed by laser, Materials Letters, 228(2018) 451-5.

[13] H. Kim, Z. Wu, N. Eedugurala, J. D. Azoulay, T. N. Ng, Solution-Processed Phototransistors Combining Organic Absorber and Charge Transporting Oxide for Visible to Infrared Light Detection, ACS Appl Mater Interfaces, 11(2019) 36880-5.

[14] H. Yoo, W. G. Kim, B. H. Kang, H. T. Kim, J. W. Park, D. H. Choi, et al., High Photosensitive Indium-Gallium-Zinc Oxide Thin-Film Phototransistor with a Selenium Capping Layer for Visible-Light Detection, ACS Appl Mater Interfaces, 12(2020) 10673-80.

[15] Y. J. Tak, D. J. Kim, W. G. Kim, J. H. Lee, S. J. Kim, J. H. Kim, et al., Boosting Visible Light Absorption of Metal-Oxide-Based Phototransistors via Heterogeneous In-Ga-Zn-O and $CH_3NH_3PbI_3$ Films, ACS Appl Mater Interfaces, 10(2018) 12854-61.